Ionic Mobility of Cation and Anion of Lithium Gel Electrolytes Measured by Pulsed Gradient Spin−Echo NMR Technique under Direct Electric Field

Hiroshi Kataoka,[†,‡] Yuria Saito,*[,†] Tetsuo Sakai,[†] Shigehito Deki,[§] and Takeyoshi Ikeda[||]

Osaka National Research Institute 1-8-31, Midorigaoka, Ikeda, Osaka 563-8577, Japan, Japan Science and Technology Corporation 4-1-8, Honcho, Kawaguchi, Saitama 332-0012, Japan, Department of Chemical Science and Engineering, Kobe University, 1-1 Rokkodai-cho, Nada, Kobe, Hyogo 657-8501, Japan, and JEOL Ltd. 3-1-2, Musashino, Akishima, Tokyo 196-0022, Japan

Received: October 31, 2000; In Final Form: January 27, 2001

The ionic mobilities of the individual cations and anions of the lithium gel electrolyte, $LiN(CF_3SO_2)_2$−EC/DEC−PVdF-HFP, were measured using the pulsed gradient spin−echo (PGSE) NMR by applying a direct electric field during the spin−echo measurements. Theoretical expressions of the echo intensity were derived by considering the effect of chemical exchange between the ion and the ion pair in the electrolyte in order to clarify the physical meaning of the experimental results. Under the potential application below 30 V, the conductivities of the lithium ion and the anion were estimated to be 3.6×10^{-5} and 9.4×10^{-5} $cm^2\ s^{-1}\ V^{-1}$, respectively. This is the first result describing the mobilities of both the cations and anions in the electrolyte that was directly measured by the combination of NMR spectroscopy and an electrochemical technique for the extraction of the individual ionic properties of migration.

Introduction

In the field of material chemistry for lithium secondary batteries, the recent development of polymer gel electrolytes has widely occurred because of their significant performance compared with that of the conventional electrolyte solution. That is, the gel could have the merits both of a liquid as high conductive electrolyte and a solid from the aspect of nonfluidity and good reliability.[1] In practice, the migration of carriers is inhibited by the polymer network in the gel compared with the carrier motion in a liquid due to the physical and chemical interactions between the carriers and the polymer.[2,3] Therefore, one of the main objectives in the investigation on the gel electrolytes directed toward the application to the lithium secondary batteries is to enhance the migration properties of lithium ions such as the transport number and conductivity.

Recently, the pulsed gradient spin−echo (PGSE) NMR technique has been effectively used to measure the diffusion coefficient of ionic species in electrolyte materials.[4] This technique has the advantage that individual chemical species can be detected, indicating the independent evaluation of the cation and the anion dynamics. Furthermore, the diffusion coefficient is correlated with the conductivity according to Einstein's relation.[5] Therefore, the measurement of the diffusion values has become one of the significant approaches during the research of ionic conduction mechanisms, especially in the solution and gel polymer electrolyte materials.[6,7]

The PGSE-NMR, however, is not sufficient to obtain the real mobility of ions which actually dominate the battery performance. This is because the diffusion coefficient is generally due to not only the ions but also the ion pairs in the electrolyte because the dissociation degree of the salt in the ordinary electrolyte is not uniform. It is impossible to distinguish the ion and the ion pair in the NMR spectra due to the fast exchange between them. Therefore, the estimated diffusion coefficients using the PGSE-NMR are simply recognized as the averaged value of the ions and the ion pairs, represented as

$$D_{obs} = \alpha D_{ion} + (1 - \alpha) D_{pair} \quad (1)$$

where α is the dissociation degree of the salt. Electrical conductivity is directly correlated not with D_{obs} but with D_{ion}, which is free from D_{pair}.

To observe the ionic motion selectively, we applied an electric field to the NMR sample system during the diffusion measurement.[8−10] Under this condition, the ions drift with a velocity, v, which is proportional to the magnitude of the applied electric field. The drift appears as a phase shift of the spin−echo signal depending on the magnitude of v and several factors of the gradient pulses.

In this report, we first derived the general expression of the spin−echo intensity for the measurement of the migration properties, including the application of the electric field on the PGSE-NMR technique. In the derivation process, the exchange effect between the ions and the ion pairs was considered. The validity of the experimental results of the ionic mobilities and the transport number could then be discussed in reference to the electrical conductivity.

Experimental Section

Samples. The gel electrolytes composed of the PVdF-type polymer were prepared by the solvent casting method as follows.

* Corresponding author. Tel. +81-727-51-9618. FAX +81-727-51-9714. E-mail saito@onri.go.jp.
[†] Osaka National Research Institute.
[‡] Japan Science and Technology Corporation.
[§] Kobe University.
[||] JEOL Ltd.

10.1021/jp0040143 CCC: $20.00
Published on Web 03/10/2001

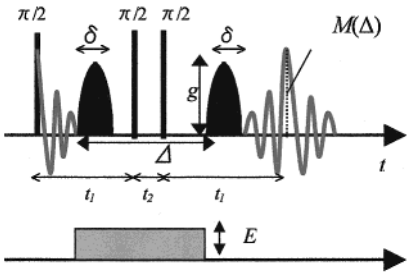

Figure 1. Stimulated echo sequence with a direct electric field. The electric field was applied to the sample during the diffusion time Δ, which is determined by the two gradient pulses.

Bistrifluoromethanesulfonimide lithium salt, $LiN(CF_3SO_2)_2$ (LiTFSI), was dissolved in the mixed solvent of ethylene carbonate (EC) and diethyl carbonate (DEC) (2/3 in volume ratio) to form a 1M solution. A small amount of copolymer poly(vinylidene fluoride−hexafluoropropylene) (PVdF-HFP, Elf Atochem Kynar 2751) was solved into acetone and then mixed with the electrolyte solution to increase the viscosity for inhibiting the thermal convection during the NMR measurements. The mixed solution was cast into a glass flask to slowly evaporate the acetone. The weight ratio of the net PVdF-HFP and the electrolyte solution was 2/98.

NMR Measurement. To measure the drift velocity of the ions and the solvent species in the gel electrolyte, we built NMR probes with the field gradient coil and electrophoretic equipment for the detection of ^{7}Li, ^{19}F, and ^{1}H as the probed nuclei of the cation and anion of the salt and the solvent species, respectively. The sample cell was composed of a cylindrical glass tube of 10 mm in diameter and two gold electrodes placed on the top and bottom of the tube supported by Teflon rings to prevent any leakage. The distance between the electrodes was kept 32 mm, and the total length of the sample was 35 mm. A direct potential was applied in a direction parallel to the static magnetic field and the gradient field. The power supply was operated at a constant voltage, reversing the polarity to inhibit the polarization and decomposition of the electrolyte material. Temperature-controlled air was flowed around the sample cell to maintain a constant temperature of 298.2 ± 0.1K during the measurement.

Spin−echo measurements were performed using a JNM-ECP300W wide-bore spectrometer (7.04 T) using the stimulated echo sequence represented in Figure 1. The $\pi/2$ pulses of the probes were 40, 45, and 25 μs for ^{7}Li, ^{19}F, and ^{1}H, respectively. The spin−lattice relaxation times, T_1, of ^{7}Li, ^{19}F, and ^{1}H in this gel were 1.8, 1.8, and 1.6 s, respectively. The half-sine-shaped gradient pulses were used because they are profitable for matching the two pulses in the sequence. Typical values of the parameters for the field gradient pulse were $g = 0.16-0.6$ T/m for the pulse strength, $\delta = 0-6$ ms for the pulse width, and $\Delta = 1-1.5$ s for the duration between the two gradient pulses. The potential in the range of 0−75 V was continuously applied from the start to the end of the spin−echo detection (1.5 s), as shown in Figure 1. A maximum applied voltage was selected from the aspect of stable measurement conditions without any anomalous change in the echo intensity and the material due to the polarization and chemical change.

The major concern that should be noted during the measurement is the heating of the sample due to the potential application. To prepare the thermal equilibrium condition of the sample, we repeated the measurement under the potential application for every ∼200 s for data integration. Inhomogeneity of the temperature in the sample often induces the thermal convection, which sensitively appears as a drastic phase rotation of the spin−echo signal during measurement, and makes it difficult to estimate the real diffusion coefficient.[11] Therefore, the localized thermal effect on the sample can be checked from this anomalous signal behavior. Ohmic heating also increases the overall sample temperature, enhancing the mobility. The temperature increase was estimated to be around 0.2 K at the maximum (25 V application for 1.5 s) for our sample from the data of the thermal capacities of the EC-, DEC-, and PVDF-type polymer.[12−14] Considering the activation energy ($E_a \approx 10$ kJ/mol of this electrolyte solution is around 298 K), this temperature change induces the variation of the mobility within 0.5%. As a result, it seems that the thermal effects due to the potential application on the sample could be neglected for our sample.

Results and Discussion

Theoretical Derivation. Experimental conditions in the measurement satisfied $\delta < t_1 \ll t_2 \approx \Delta$. Therefore, the echo intensity, $M(2t_1 + t_2) \cong M(\Delta)$, observed during the diffusion measurement by applying two equivalent field gradient, is generally expressed as follows

$$M(\Delta) = M_0 \exp(-q^2 D\Delta) \tag{2}$$

$$q = 2\gamma\delta g\pi^{-1} \tag{3}$$

where γ is the gyromagnetic ratio of the nucleus, δ is the width of the field gradient pulse, g is the maximum strength of the field gradient pulse, Δ is the duration between the pulses, corresponding to the diffusion time, and D is the diffusion coefficient of the nuclear species.[15] Coherent motion along the field gradient characterized by a constant drift velocity due to some additional flow produces a phase shift in the echo signal. When both the diffusion and flow contribute to the translational motion of the species, the echo response follows the relation

$$M_v(\Delta) = M_0 \exp(iq\nu\Delta - q^2 D\Delta) \tag{4}$$

where ν is the drift velocity of the flow and i is the imaginary unit, $i = \sqrt{-1}$.[8] We can derive ν using the ratio of the echo intensities with and without the drift

$$M_v/M = \exp(iq\nu\Delta) \tag{5}$$

When the flow is attributed to a direct electric field, E, applied on the electrolyte material, only the charged ionic species respond to the field effect and move. As a result, the ionic mobility, μ, could be derived from the relation

$$\mu = \nu/E \tag{6}$$

Here, we consider the equilibrium state of the electrolyte material in which the dissociated ions and undissociated ion pairs coexist as

$$LiN(CF_3SO_2)_2 \leftrightarrow Li^+ + N(CF_3SO_2)_2^- \tag{7}$$

The dissociation degree of the salt depends on solution properties such as the solution concentration, viscosity, dielectric constant, and solvation effect. When we assume that the lifetimes of the

ion and the ion pair in the solution are τ_{ion} and τ_{pair}, respectively, the spin−echo of each component is attenuated[10,16,17] as

$$\frac{d}{d\Delta}M_{ion} = (-D_{ion}q^2 + iq\nu_{ion})M_{ion} + \frac{1}{\tau_{pair}}M_{pair} - \frac{1}{\tau_{ion}}M_{ion} \quad (8)$$

$$\frac{d}{d\Delta}M_{pair} = (-D_{pair}q^2)M_{pair} - \frac{1}{\tau_{pair}}M_{pair} + \frac{1}{\tau_{ion}}M_{ion} \quad (9)$$

or

$$\frac{d}{d\Delta}\begin{bmatrix}M_{ion}\\M_{pair}\end{bmatrix} = \frac{d}{d\Delta}M = LM \quad (10)$$

where

$$\mathrm{L} = \begin{bmatrix} -\frac{1}{\tau_{ion}} + iq\nu_{ion} - D_{ion}q^2 & \frac{1}{\tau_{pair}} \\ \frac{1}{\tau_{ion}} & -\frac{1}{\tau_{pair}} - D_{pair}q^2 \end{bmatrix} \quad (11)$$

The lifetime of each species is correlated with the probability of existence, p_{ion} and p_{pair}, in the form

$$p_{ion} = \frac{\tau_{ion}}{\tau_{pair} + \tau_{ion}} \qquad p_{pair} = 1 - p_{ion} \quad (12)$$

The imaginary component, $iq\nu_{ion}$ in eq 11 represents the flow of the charged species according to the electric field. The total spin−echo intensity can be expressed as

$$M = M_{ion} + M_{pair} = M_0[a_1 \exp(-\alpha_1\Delta) + a_2 \exp(-\alpha_2\Delta)] \quad (13)$$

where

$$2\alpha_{1(2)} = q^2D_{pair} + q^2D_{ion} - iq\nu_{ion} + \frac{1}{\tau_{pair}} + \frac{1}{\tau_{ion}} \mp \left[\left(q^2(D_{ion} - D_{pair}) + \left(\frac{1}{\tau_{ion}} - \frac{1}{\tau_{pair}}\right) - iq\nu_{ion}\right)^2 + \frac{4}{\tau_{pair}\tau_{ion}}\right]^{1/2} \quad (14)$$

$$a_1 = 1 - a_2 \quad (15)$$

$$a_2 = \frac{1}{\alpha_2 - \alpha_1}[p_{pair}q^2D_{pair} + p_{ion}(q^2D_{ion} - iq\nu_{ion}) - \alpha_1] \quad (16)$$

When the chemical exchange between the ion and the ion pair is slow, which corresponds to the condition, $(D_{ion(pair)}q^2)^{-1} \ll \tau_{ion(pair)}$, the real part of eq 13, the observed echo intensity, can be summarized as

$$\mathrm{Re}M = \mathrm{Re}M_0[p_{pair}\exp(-q^2D_{pair}\Delta) + p_{ion}\exp(iq\nu_{ion}\Delta - q^2D_{ion}\Delta)]$$
$$= M_0[p_{pair}\exp(-q^2D_{pair}\Delta) + p_{ion}\cos(q\nu_{ion}\Delta)\exp(-q^2D_{ion}\Delta)] \quad (17)$$

This shows that the echo intensity consists of two components, the diffusing ion pairs and the diffusing ions also drifting in response to the electric field. Figure 2a shows a schematic diagram of eq 17 as a function of δ. This is the case when the ions and the ion pairs exist almost independently, such as the solution composed of a dissociative salt and an undissociative salt.

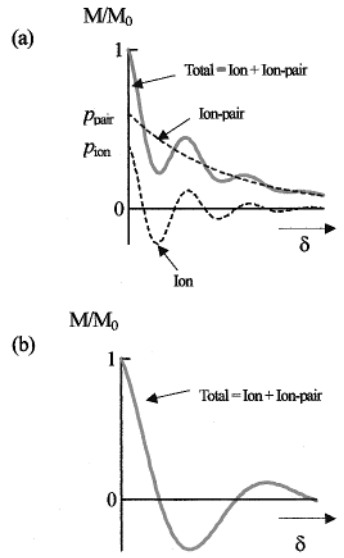

Figure 2. Schematic diagrams of the dependence of the echo intensity, M/M_0. (a) The case of slow exchange between the ions and the ion pairs. The total intensity consists of the ion pair component of diffusing and the ion component of diffusing and drifting. (b) The case of fast exchange between the ions and the ion pairs. The total intensity consists of the averaged values of the ions and ion pairs.

When the exchange between the ions and the ion pairs is fast, satisfying the condition, $(D_{ion(pair)}q^2)^{-1} \gg \tau_{ion(pair)}$, eq 13 can be abbreviated as

$$\mathrm{Re}\,M = M_0\cos(q\nu_{a\nu}\Delta)\exp(-q^2D_{a\nu}\Delta) \quad (18)$$

where

$$D_{a\nu} = p_{pair}D_{pair} + p_{ion}D_{ion} \quad (19)$$

$$\nu_{a\nu} = p_{ion}\nu_{ion} \quad (20)$$

Thus, we could present

$$\mu_{a\nu} = p_{ion}\mu_{ion} \quad (21)$$

This description represented in Figure 2b shows the characteristics of a single-exponential function. The apparent diffusion coefficient, $D_{a\nu}$, is the mean value of the diffusion coefficients of the ion and the ion pair. Further, it should be noted in eqs 20 and 21 that the estimated drift velocity and mobility from the experimental results definitely includes the ionic probability of existence factor. In the conventionally used electrolyte solutions and gel polymer electrolytes under equilibrium conditions, the chemical exchange between the ions and the ion pairs would be fast compared with the time taken for a measurement of the chemical and/or physical properties. That is, we can observe the averaged existence condition of the object. For example, the electrical conductivity measured by the impedance technique could be recognized as a response by the mobile ions. However, the ions change to the immobile ion pairs for the period of p_{pair} of the total measuring time. Therefore, the conductivity represents the migration feature of the ions reflecting the probability of existence.

Equation 21 precisely represents this situation. As a result, the estimated mobility, $\mu_{a\nu}$, using the NMR technique by the application of the direct electric field shows the different meaning of the mobility, μ_e, in the factor of the conductivity which represents the mobility of the isolated ions.

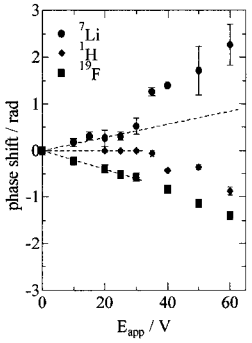

Figure 3. Applied potential dependence of the phase shift of the echo signals of the cation, anion, and solvent species probed by ^{7}Li, ^{19}F, and ^{1}H, respectively under the experimental condition of $\delta = 1.8$ ms, $\Delta = 1.5$ s, $g(^7\text{Li}) = 0.6$ T/m, and $g(^{19}\text{F},^1\text{H}) = 0.16$ T/m. The straight line is the linear fit of the experimental data of ^{7}Li until 30 V.

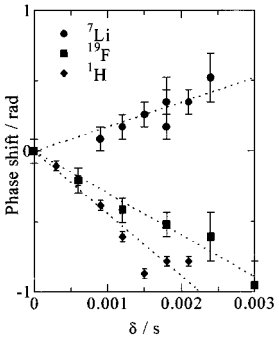

Figure 4. Gradient pulse width, δ, dependence of the phase shift of the echo signals under the experimental condition of $\Delta = 1.5$ s, $g(^7\text{Li}) = 0.6$ T/m, $g(^{19}\text{F},^1\text{H}) = 0.16$ T/m, applied potential $V(^7\text{Li},^{19}\text{F}) = 25$ V, and applied potential $V(^1\text{H}) = 60$ V.

Experimental Evaluation. Figure 3 shows the applied potential dependence of the phase value of the NMR spin−echo in eq 5. The phase of ^{19}F decreased almost linearly with the potential in the measurement region. On the other hand, the phase of ^{7}Li increased opposite to the ^{19}F behavior with increasing voltage. This means that the cations probed by ^{7}Li and the anions probed by ^{19}F drifted to the cathode and the anode, respectively, in response to the applied direct electric field. The slope of the phase change of ^{7}Li increased at ~30 V application. This indicates that the mobility of the cation was enhanced under the applied voltage above 30 V. In the case of ^{1}H, both peaks from EC and DEC showed the same behaviors under the measurement conditions. The signal phase did not change under the potential below ~30 V and decreased linearly with the voltage above 30 V. These anomalous features of ^{7}Li and ^{1}H at above 30 V reflect an additional drift effect which is independent of the electric field effect on the charged species represented by eq 6.

The δ dependence of the phase value of the spin−echo response for each nuclear species was plotted in Figure 4 to estimate the mobility according to eqs 5 and 6. Considering the potential dependence of the phase in Figure 3, we applied 25 V of potential for the ^{7}Li and ^{19}F measurements because it induces the drift of the charged species in proportion to the electric field. Also, 60 V was applied for the detection of ^{1}H phase change as a function of δ to estimate the apparent mobility due to some driving force different from the electric field. The estimated values of the ionic mobilities and lithium ion transport number are shown in Table 1.

The mobility obtained from this method includes the probability of existence of the ions (p_{ion}) according to eq 21. p_{ion} corresponds to the dissociation degree of the salt (α) when we consider the equilibrium state of the solution. The electrical conductivity σ, therefore, is expressed using α

$$\sigma = \mu_e ne = \mu_e(\alpha N)e = (\alpha\mu_e)Ne = p_{ion}\mu_e Ne \qquad (22)$$

where μ_e is the mobility component of the charged species in the conductivity and n is the net ionic concentration which is expressed by the solution concentration, N, multiplied by α. From the impedance result of this sample, we could estimate $p_{ion}\mu_e \approx 3.8 \times 10^{-5}$ cm^2 s^{-1} V^{-1}. This is around one-third of the total mobility obtained from the NMR results. The difference between the mobility values would be due to the correlation factor, which plays part connecting the diffusion coefficient and the electrical conductivity in the Nernst−Einstein equation.[18] Essentially, it can be realized that the estimated values using the NMR technique with the potential application are reasonable as the ionic mobilities in comparison with the values of the lithium ions in aqueous solutions.[8]

TABLE 1: Mobility of the Cation, Anion, and Solvent Species Probed by ^{7}Li, ^{19}F, and ^{1}H, Respectively

$\mu(Li^+)$	3.6×10^{-5} cm^{2}s^{-1}V^{-1}
$\mu(N(CF_3SO_2)_2^-)$	9.4×10^{-5} cm^{2}s^{-1}V^{-1}
$t(Li^+)$	0.28

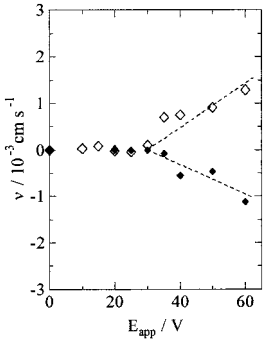

Figure 5. Applied potential dependence of the drift velocity of the cation (◇) and the solvent species (♦), which correspond to the deviation of the experimental data from extrapolated experimental data lined in Figure 3.

To discuss the reason of the anomalous change in the mobilities of ^{7}Li and ^{1}H at above 60 V, changes in the drift velocity with the applied potential were plotted in Figure 5 for the cation and the solvent species. Each mark gives the deviation of the experimental value from the extrapolated experimental value until 30 V, corresponding to the dashed line in Figure 3. The slope of the dashed line of ^{1}H in Figure 5 reflects the apparent mobility of $\mu_{app} \approx 1.0 \times 10^{-4}$ cm^2 s^{-1} V^{-1}. The slope of the additional component of ^{7}Li (dashed line) also gives the apparent mobility of $\sim 1.5 \times 10^{-4}$ cm^2 s^{-1} V^{-1}. The fact that the increased mobility of the cation is almost compatible with that of the solvent species under the higher voltage application can be explained as follows. Under voltages higher than the decomposition potential, the lithium tends to be deposited at the cathode surface. This results in the exhaustion of the lithium ions in the vicinity of the electrode, forming a concentration gradient of lithium in the electrolyte. This situation would accelerate the transport of lithium from the center to the deposited region near the electrode. Consequently, the solvent species are driven behind the lithium, indicating the same drift velocity in opposite direction.

It is possible that the additional movement of the solvent species and the cations is due to the inhomogeneity of the direct electric field. It seems that three phenomena are significantly

responsible for this situation. One is the potential drop at the electrode/electrolyte interface during the potential application. As a result, a fraction of the applied potential (not the total of it) appears across the electrolyte. To obtain the net value of the electric field on the electrolyte, one should insert another couple of electrodes in the electrolyte different from the electrodes for the potential application. Furthermore, the current will decay with time from an initial value to zero when blocking electrodes are used for drifting ions. This means that the applied electric field is not precisely constant during the measurement. However, this problem was not very serious under our measurement conditions, in which the time for continuous potential application was 1.5 s. To prepare a more precise condition for constant current flow using the blocking electrodes, we could apply the potential by keeping the detected current constant. Another approach is to use reversible electrodes for lithium ions, such as lithium metal. The final issue, which disturbs the steady state in the electrolyte, is the polarization and/or the chemical change of the electrolyte from the potentials' electric effect. In particular, these phenomena appear in the vicinity of the electrodes and at higher potential applications. To restrict any change in the quality of the electrolyte, we altered the polarity of the applied voltage for every one step of the echo detection. Improvement of these problems are now in progress to confirm the absolute values of the mobility and the reason for the solvent drifting.

Conclusion

The individual ionic mobilites of the lithium gel electrolyte, $LiN(CF_3SO_2)_2$−EC/DEC−PVDF-HFP, were measured using the pulsed gradient spin−echo NMR with the application of a direct electric field. The mobilities of the lithium ion and the anion were 3.6×10^{-5} and 9.4×10^{-5} $cm^2\ s^{-1}\ V^{-1}$, respectively. Theses values are consistent with the mobility estimated from the electrical conductivity. A drift in the solvent species was detected using the ^1H probe under the higher electric field. The apparent mobility of the solvent species was $\sim 1.0 \times 10^{-4}$ $cm^2\ s^{-1}\ V^{-1}$. This value is comparable to the increased mobility of the cation, $\sim 1.5 \times 10^{-4}$ $cm^2\ s^{-1}\ V^{-1}$, detected under the applied potential above 30 V. It could be speculated that the change in the drift velocity (ionic mobility) under the applied voltage above 30 V is due to the flow of the lithium to compensate the lithium deposition at the electrode surface. This change results in the flow of the solvent species against the cations.

References and Notes

(1) Abraham, K. M. In *Application of Electroactive Polymers*; Scrosati, B., Ed.; Chapman & Hall: London, 1993; p175.
(2) Saito, Y.; Kataoka, H.; Capiglia, C.; Yamamoto, H. *J. Phys. Chem. B* **2000**, *104*, 2189.
(3) Qureshi, M. Y.; Berstan, D.; Cameron, G. G.; Ingram, M. P.; Rousselot, C. *Polym. Int.* **1998**, *47*, 16.
(4) Price, W. S. *Annu. Rep. NMR Spectrosc.* **1996**, *32*, 51.
(5) Atkins, P. W. *Physical Chemistry*, 6th ed.; Oxford University Press: New York, 1998; p 749.
(6) Clericuaio, M.; Parker, W. O., Jr.; Soprani, M.; Andrei, M. *Solid State Ionics* **1996**, *82*, 179.
(7) Fleischer, G.; Scheller, H.; Kärger, J.; Reiche, A.; Sandner, B. *J. Non-Cryst. Solids* **1998**, *742*, 235.
(8) Holz, M. *Chem. Soc. Rev.* **1994**, 165.
(9) Dai, H.; Zawodzinski, T. A. Jr. *J. Electroanal. Chem.* **1998**, *459*, 111.
(10) Johnson, C. S., Jr. *Prog. NMR Spectrosc.* **1999**, *34*, 203.
(11) Kataoka, H.; Saito, Y.; Sakai, T.; Quartarone, E.; Mustarelli, P. *J. Phys. Chem. B* **2000**, *104*, 11460.
(12) Peppel, W. J. *Ind. Eng. Chem.* **1958**, *50*, 767.
(13) Kolosovskii, N. A.; Udovenko, W. W. *Zh. Obshchei Khim.* **1934**, *4*, 1027.
(14) KYNAR catalog, Elf Atochem Japan.
(15) Price, W. S.; Hayamizu, K.; Ide, H.; Arata, Y. *J. Magn. Reson.* **1999**, *139*, 205.
(16) Zimmerman, J. R.; Brittin, W. E. *J. Phys. Chem.* **1957**, *61*, 1328.
(17) Kärger, J.; Pfeifer, H.; Heink, W. *Adv. Magn. Reson.* **1988**, *12*, 1.
(18) West, A. R. *Solid State Chemistry and its Applications*; John Wiley & Sons: New York, 1985; p 462.